

PACS numbers: 05.70.Ce, 06.60.Vz, 61.66.Dk, 64.75.Nx, 65.40.gd, 81.20.Vj, 82.60.Cx

## **Influence of Adhesive-Active Components on Thermodynamic Parameters of High-Entropy NiCoCrAl–(Ti, Nb) Brazing Filler Metals**

S. V. Maksymova, V. V. Voronov, and P. V. Kovalchuk

*E. O. Paton Electric Welding Institute, N.A.S. of Ukraine,  
11 Kazymyr Malevych Str.,  
UA-03150 Kyiv, Ukraine*

The conventional practice of heat-resistant nickel-alloys' brazing involves the utilization of industrial Ni–Cr–(B, Si)-based filler metals. However, employing filler metals within this system results in the formation of brittle compounds, specifically, silicides and borides of nickel, chromium, and other elements. These brittle phases have the potential to diminish the mechanical characteristics of brazed assemblies. This study investigates the feasibility of developing multicomponent high-entropy filler metals for brazing Ni-based alloys (specifically, heat-resistant ones) without including boron and silicon in their composition. Utilizing computational methods and the updated Hume-Rothery rules, we identified a promising NiCoCrAl–(Ti, Nb) system. Various thermodynamic parameters are computed, and corresponding dependences on the alloying-components' content are established. The alloying limits of experimental alloys are determined, aligning with the criteria established for high-entropy alloys (HEA). Melting temperatures are calculated, and the liquidus-surface area of the NiCoCrAl–(Ti, Nb) system is delineated. Based on the research findings, it is determined that this alloy possesses a dendritic structure with some amount of eutectic component, and its melting temperature below 1220°C makes it suitable for brazing heat-resistant nickel alloys.

**Key words:** high-entropy alloy, brazing filler metal, brazing, nickel-based alloys, entropy of mixing, enthalpy of mixing, titanium, niobium.

---

Corresponding author: Svitlana Vasylyvna Maksymova  
E-mail: maksymova@kiev.paton.ua

Citation: S. V. Maksymova, V. V. Voronov, and P. V. Kovalchuk, Influence of Adhesive-Active Components on Thermodynamic Parameters of High-Entropy NiCoCrAl–(Ti, Nb) Brazing Filler Metals, *Metallofiz. Noveishie Tekhnol.*, **46**, No. 8: 811–823 (2024). DOI: [10.15407/mfint.46.08.0811](https://doi.org/10.15407/mfint.46.08.0811)

Звичайною практикою під час лютування жароміцних ніклевих стопів є використання промислових прилюток системи Ni–Cr–(B, Si). Проте використання прилюток такої системи призводить до утворення крихких сполук — силіцидів і боридів Ніклю, Хрому й інших елементів, які можуть понижувати механічні характеристики паяних з'єднань. У представленій роботі досліджується можливість створення багатокомпонентних високоентропійних прилюток для лютування ніклевих стопів (у тому числі жароміцних), що не містять у своєму складі Бору та Силіцію. З використанням розрахункових методик і модернізованих критеріїв Юм-Розері визначено перспективну систему NiCoCrAl–(Ti, Nb), розраховано низку термодинамічних параметрів і побудовано відповідні залежності від вмісту легувальних компонентів системи. Визначено граничні межі легування експериментальних стопів, в яких значення даних термодинамічних величин відповідають критеріям, які висуваються до високоентропійних стопів (ВЕС). Розрахунковим шляхом визначено температури топлення та побудовано ділянку поверхні ліквідусу системи NiCoCrAl–(Ti, Nb). За результатами розрахунків для проведення подальших експериментів обрано стоп  $Ni_xCoCrAlTi_yNb_z$ . За результатами досліджень встановлено, що даний стоп має дендритну структуру з невеликою кількістю евтектичної складової, а температура топлення є нижчою за 1220°C, що робить його придатним для лютування жароміцних ніклевих стопів.

**Ключові слова:** високоентропійний стоп, прилюток, лютування, ніклеві стопи, ентропія змішання, ентальпія змішання, Титан, Ніобій.

*(Received 5 March, 2024; in final version, 11 April, 2024)*

## 1. INTRODUCTION

Due to their remarkable resistance to oxidation and corrosion at elevated temperatures, as well as high strength and deformation resistance under extreme conditions, heat-resistant nickel alloys have become integral in the manufacturing of turbine components, combustion chamber compartments, and other critical parts for aviation and power applications. Notably, brazing stands out as the primary method for joining dispersion-hardening cast heat-resistant nickel alloys on a nickel base [1, 2]. Achieving high oxidation/corrosion resistance, enhanced creep resistance, and maintaining microstructure stability are imperative requirements for the success of brazed joints [1, 3].

Existing brazing filler metals are predominantly developed within the nickel–chromium (Ni–Cr) system, further optimized by incorporating a comprehensive set of alloying elements [1, 3]. Additionally, melting-point depressant elements (MPD), such as boron and silicon, are commonly introduced into these systems [1, 3–7].

Brazed joints formed using Ni–Cr filler metals consist of three distinct phases: a  $\gamma$ -hard nickel-based solution at the ‘brazed seam–base

metal' interface, chromium and nickel borides along the grain boundaries of the base metal, and eutectics primarily positioned along the seam axis. These eutectics comprise silicides and borides of nickel, chromium, and other boride-forming elements. The presence of these brittle phases within the brazed seam significantly influences the overall assembly fragility [3, 6, 8–10].

In recent years, extensive research has been conducted to address the challenges posed by the formation of fragile layers in brazed joints. High-entropy alloys (HEA) have emerged as a promising alternative as filler metals in these applications [1, 3, 11, 12].

Difficulties in developing high-entropy filler metals stem from challenges associated with chemical composition, microstructure, the necessity of achieving optimal wetting on specific base metals, and ensuring desired performance characteristics of brazed joints. An essential parameter in this context is the melting temperature of filler metals, which must not surpass the autonomous melting temperature of the base metal to preserve its original structure and, consequently, its physical and mechanical properties [13].

The exploration of HEA as filler metals for joining Ni-based alloys is currently in its early stages. Initial efforts have predominantly focused on the utilization of transition-metal HEA, akin to or derived from Cantor's alloy (an equiatomic alloy of the CoCrFeMnNi system [14]). These alloys can be further enriched with elements such as Ge, Sn, and Ga to achieve the required brazing temperature, ensure effective wetting of the base material, and enhance the quality of brazed joints [1, 15, 16, 17].

High-entropy alloys are defined as metal alloys containing 5 or more chemical components, each present in the composition at 5 to 35 at.%. These alloys exhibit a distinctive feature of preferentially forming disordered solid solutions, stabilized by a high entropy of mixing ( $\Delta S_m \geq 1.5R$ ) [1, 3, 18–21]. It is hypothesized that in the liquid state, these melts act as atomic solutions, transitioning into multicomponent hard alloys upon crystallization. The increased entropy of such melts, resulting from the numerous components, facilitates the formation of solid solutions with a random atomic distribution, preventing the formation of intermetallic phases during crystallization [20, 21].

The presence of heterogeneous atoms from elements with diverse electronic structures, sizes, and thermodynamic properties in the crystal lattice of a solid substitution solution induces significant distortion. This distortion contributes to notable solid solution strengthening and the thermodynamic stability of properties. Simultaneously, the reduced free energy of HEA ensures the stability of the solid solution during potential subsequent heat treatments [18, 20].

However, a high value of entropy  $\Delta S_m$  does not universally guarantee the formation of solid solutions. Numerous studies have revealed

that alloys with high entropy may not necessarily exhibit the structure of a disordered solid solution. On one hand, an increase in the number of alloying elements tends to enhance the likelihood of solid solution formation; however, in many cases, the outcome includes the formation of ordered phases, complex intermetallic compounds, or even amorphous phases [13, 22–25].

An analysis of high-entropy alloy properties underscores that multiphase high-entropy systems often present a more favourable combination of mechanical characteristics, encompassing including yield and tensile strength, as well as ductility [13]. Eutectic high-entropy alloys, for instance, not only ensure high mechanical properties through a fine distribution of phases but also exhibit good fluidity and a reduced propensity for component segregation during melting, which is quite often noted in conventional HEA [26–30].

These features lay the groundwork for the development of alloys with a desired combination of properties, including high hardness, wear resistance, at both normal temperatures and elevated ones, and resistance to oxidation.

The primary objective of this study was to formulate a high-entropy alloy suitable for use as a filler metal for brazing Ni-based alloys, guided by criteria for phase formation in high-entropy alloys as well as the results of statistically processed thermodynamic parameters.

## 2. MATERIALS AND METHODS

### 2.1. Calculation Methodology

The chosen filler metal system is based on the Ni–Co–Cr–Al alloy. This base system was further enriched with titanium and/or niobium to achieve the necessary liquidus temperature and enhance heat resistance and strength by promoting the formation of the requisite volume fraction of the strengthening  $\gamma'$ -phase  $\text{Ni}_3(\text{Al}, \text{Ti}, \text{Nb})$ .

The prediction of properties and structure for the experimental NiCoCrAl–(Ti, Nb) alloys of the employed criteria for phase formation in high-entropy alloys based on modified Hume-Rothery rules and several thermodynamic parameters [20, 31–36] as follow.

*Entropy of mixing* ( $\Delta S_m$ )

$$\Delta S_m = -R \sum_{i=1}^n c_i \ln(c_i), \quad (1)$$

where  $n$  is the number of alloy components;  $c_i$  is the concentration of the  $i$ -th alloying element;  $R$  is the universal gas constant.

If we consider the content of one of the elements in the alloy, such as nickel (Ni) in our case, as  $c_x$  and assume equiatomic concentrations of the remaining elements, Eq. (1) takes the form:

$$\Delta S_m = -R \left[ c_x \ln(c_x) + c_x \ln\left(\frac{1-c_x}{n-1}\right) \right]. \quad (2)$$

*Enthalpy of mixing*

$$\Delta H_m = \sum_{\substack{i=1 \\ j=1}}^n 4\Delta H_{ij}^{AB} c_i c_j, \quad (3)$$

where  $\Delta H_{ij}$  is the mixing enthalpy of the binary equiatomic  $ij$  alloy;  $c_{i(j)}$  is the concentration of the  $i$ -th ( $j$ -th) component.

*Atomic radii mismatch coefficient*

$$\delta = 100 \sqrt{\sum_{i=1}^n c_i \left(1 - \frac{r_i}{\bar{r}}\right)^2}, \quad (4)$$

where  $r_i$  is the atomic radius of the  $i$ -th element and  $\bar{r}$  is the average atomic radius:

$$\bar{r} = \sum_{i=1}^n c_i r_i. \quad (5)$$

*Generalized thermodynamic parameter*

$$\Omega_m = \frac{T_m S_m}{|\Delta H_m|}, \quad (6)$$

where  $T_m$  is the average melting temperature of the multicomponent system:

$$T_m = \sum_{i=1}^n c_i T_i. \quad (7)$$

*Valence electron concentration (VEC<sub>m</sub>)*

$$VEC_m = \sum_{i=1}^n c_i VEC_i, \quad (8)$$

where  $VEC_i$  is the valence electron concentration of the  $i$ -th element.

*Phase composition prediction parameter [37]*

$$\Lambda_m = \frac{\Delta S_m}{\delta^2}. \quad (9)$$

To ascertain the liquidus temperature of alloys and the impact of alloying elements on it, expressions based on the Taylor and Maclaurin series' expansion of the concentration dependence of solid and liquid temperatures on corresponding multidimensional surfaces [38] were employed:

**TABLE 1.** Physical properties of the alloy components [31].

Element	Atomic radius $r$ , Å	Pauling electronegativity	Melting point $T_L$ , K	Concentration of valence electrons $VEC$ , e/at.
Ni	1.25	1.91	1728	10
Co	1.25	1.88	1768	9
Cr	1.25	1.66	2136	6
Al	1.43	1.61	933	3
Ti	1.47	1.54	1941	4
Nb	1.43	1.6	2750	5

**TABLE 2.** Enthalpy of mixing of binary systems, kJ/mole [39].

Element	Ni	Co	Cr	Al	Ti	Nb	Ta
Ni	—	0	-7	-22	-35	-7	-29
Co	0	—	-4	-19	-28	-5	-24
Cr	-7	-4	—	-10	-7	-7	-7
Al	-22	-19	-10	—	-30	-18	-19
Ti	-35	-28	-7	-30	—	2	1
Nb	-7	-5	-7	-18	2	—	0

$$T_{\text{liq}} = T_{\text{liq}}^{\text{Ni}} + \sum_{i=1} \left( \frac{dT_{\text{Ni}}}{dT_i} \right) c_i, \quad (10)$$

where  $dT_{\text{Ni}}/dT_i$  is the tangent of the angle of inclination of the tangential to the liquidus line drawn from the melting point of pure nickel on the corresponding binary diagrams. These values typically fall within the limits of a solid solution, where the segment of the solidus curve closely approximates a straight line [38].

The primary data used during the calculations are given in Table 1 and Table 2.

The obtained calculation data underwent subsequent statistical analysis.

## 2.2. Structural Characterization

The selected experimental alloys were fabricated from pure components through argon-arc melting with a non-fusible tungsten electrode on a water-cooled copper substrate in a high-purity argon environ-

ment. To ensure uniform alloying element distribution, the ingot underwent five successive remeltings.

Metallographic studies and micro-x-ray spectral analysis were conducted on samples post-determination of the melting temperature range, with all alloys cooled to room temperature at the same rate. Samples were prepared according to standard methods, and their microstructure was examined using a Tescan Mira 3 LMU scanning electron microscope. Local micro-x-ray spectral analysis, employing an Oxford Instruments X-max 80-mm<sup>2</sup> energy dispersive spectrometer, was utilized to study element distribution in distinct phases.

### 3. RESULTS AND DISCUSSION

Throughout the research, various thermodynamic parameters of NiCoCrAl–(Ti, Nb) alloy systems with different component ratios were calculated.

Equation (2) was employed to establish the relationship between parameter ( $\Delta S_m/R$ ) and the content of the base element (nickel in this case) for  $n$ -element multicomponent alloys, as depicted in Fig. 1.

The data reveal that for the content of the base component within the range of 5 at.% to 35 at.%, and with equiatomic content of the remaining alloy elements, the enthalpy of mixing  $\Delta S_m \geq 1.5R$  across the entire studied area.

However, as previously noted, a high  $\Delta S_m$  value does not ensure the

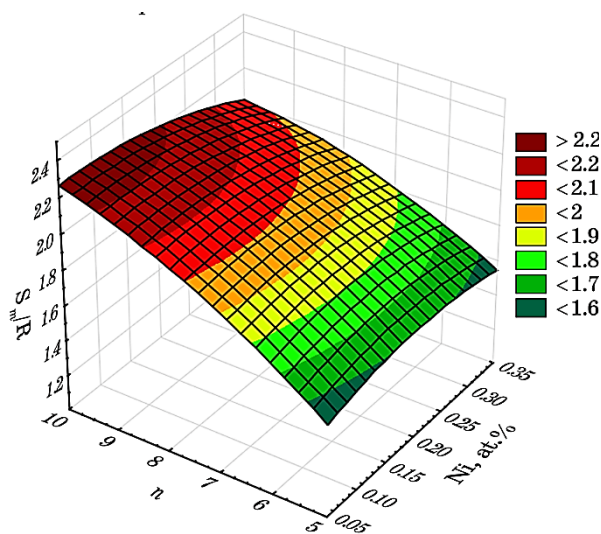


**Fig. 1.** Calculation results of the parameter  $\Delta S_m/R$  depending on the content of the base element (nickel) for  $n$ -element multicomponent alloys.

formation of solid solutions.

To gain a more profound insight into the formation processes of high-entropy alloys and their potential design, creation, and property prediction, it becomes essential to investigate other factors such as the atomic radii mismatch ( $\delta$ ), enthalpy of mixing ( $\Delta H_m$ ), thermodynamic parameter ( $\Omega$ ), valence-electrons' concentration ( $VEC$ ) and geometric parameter ( $\Lambda$ ) [9, 13, 19–32].

The calculated of atomic radii mismatch ( $\delta$ ) for all alloys did not exceed 6.0% to 7.7%. It is worth noting that, according to the literature, this value should not exceed 8.5–12% to obtain the structure of a solid solution in high entropy alloys [38].

One of the leading factors in the formation of the structure of high-entropy alloys is the enthalpy of mixing [31, 40, 41].

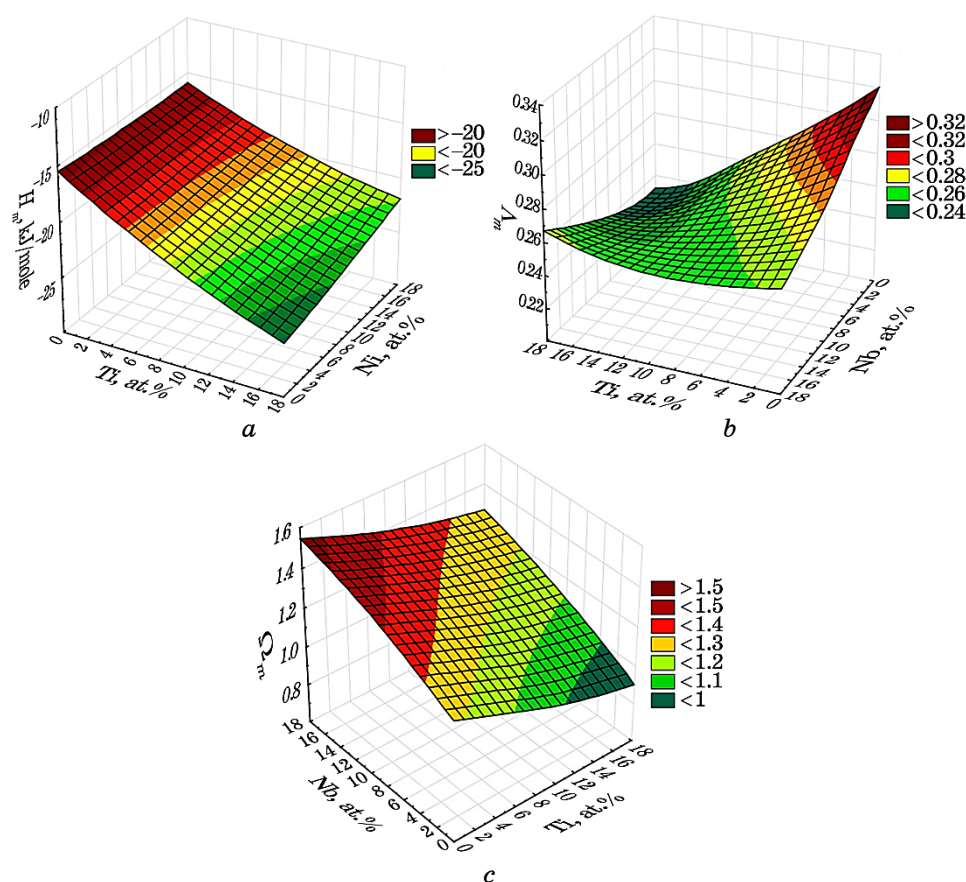


**Fig. 2.** Calculation results of the enthalpy of mixing  $\Delta H_m$  (a), the size parameter  $\Lambda_m$  (b) and the generalized thermodynamic parameter  $\Omega_m$  (c) depending on the content of NiCoCrAl–(Ti, Nb) alloy components.



The evaluation of the calculated data obtained for alloys of the NiCoCrAl–(Ti, Nb) system shows that alloying with titanium leads to a significant decrease in the value of the mixing enthalpy, while doping with niobium has almost no effect on the value of  $\Delta H_m$  (Fig. 2, *a*). Thus, simultaneous codoping with these two elements allows obtaining the value of  $\Delta H_{\text{mix}}$  in the region recommended for HEA ( $-22 \leq \Delta H_{\text{mix}} \leq 7$  kJ/mol [31]).

Despite the significant role of enthalpy in the formation of the structure of high-entropy alloys, for a more accurate prediction of the formation of the phase composition, it is recommended to use the parameter  $\Lambda_m$ . This calculated parameter indicates that an increase in entropy  $\Delta S_m$  contributes to the formation of a solid solution; while an increase in the difference in atomic radii  $\delta$  prevents this one (the value of  $\delta^2$  is proportional to the deformation of the crystal lattice in the system). According to literature data [37], at values of the parameter  $\Lambda_m > 0.96$ , an ordered solid solution should form in the alloy, and at  $\Lambda_m < 0.24$ , ordered compounds and intermetallic phases are formed.

Based on the calculation results, it was established that doping the alloy with titanium in the range of 0–18 at.% significantly decreases the  $\Lambda_m$  parameter to values of  $\Lambda_m < 0.24$  (Fig. 2, *b*). This combined with a substantial decrease in the enthalpy of mixing (to 22–25 kJ/mol), indicates a high probability of the formation of ordered compounds and intermetallic in the alloys.

On the other hand, when doping with niobium, this parameter is in the range of 0.26–0.28, which, combined with the insignificant influence of niobium on the change in the mixing enthalpy, may indicate a high probability of the formation of a mixed structure in this case.

Simultaneous codoping with titanium and niobium allows, on one hand, to maintain the value of the parameter  $\Lambda_m$  within 0.26–0.28 while keeping the mixing enthalpy  $\Delta H_m$  at the level of 15–16 kJ/mol. According to literature data, at such values of thermodynamic parameters, a mixed structure of several solid solutions should theoretically form in the alloy. At the same time, the generalized thermodynamic parameter  $\Omega_m$  for these alloys is at the level of  $\Omega_m = 1.1$ –1.5 (Fig. 2, *c*), confirming the possibility of the formation of a mixed structure in these alloys.

The lattice type of such solid solutions can be predicted using the  $VEC_m$  parameter. According to the Hume-Rothery rule, the valence electron concentration ( $VEC$ ) predicts the type of crystal lattice [31, 41–43]. At  $VEC_m \geq 8.0$ , a single-phase f.c.c. structure should form, while at  $6.87 \leq VEC_m < 8.0$ , b.c.c. and f.c.c. phases coexist, and at  $VEC_m < 6.87$ , a single-phase b.c.c. structure takes place [31, 44].

Analysis of selected experimental alloys revealed that, with separate alloying with titanium and niobium in the NiCoCrAl–(Ti, Nb) system alloys, the value of  $VEC_m$  for NiCoCrAl–Ti and NiCoCrAl–Nb alloys is

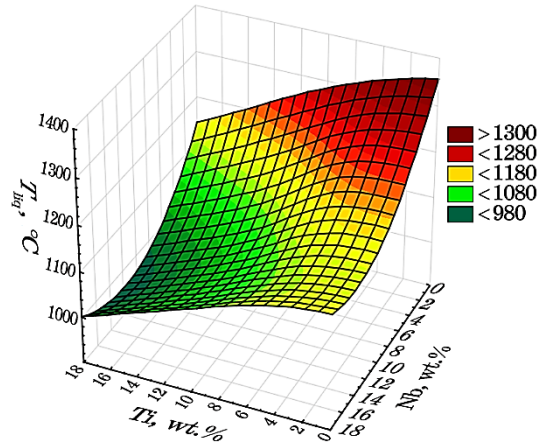


Fig. 3. Calculated liquidus surface of the NiCoCrAl–(Ti, Nb) alloys.

TABLE 3. Calculated thermodynamic parameters of the selected NiCoCrAl–(Ti, Nb) alloy.

$\Delta H_m$ , kJ/mole	$\Delta S_m$ , J/mole	$\Omega_m$	$\delta_m$ , %	$VEC_m$	$\Lambda_m$	$T_{liq}$ , °C
-21.12	-1.64*R	1.1	7	7.15	0.28	1215

within 6.4–6.6 range, indicating the formation of a solid solution with a b.c.c. lattice. In turn, with simultaneous doping, depending on the component ratio, the value of this parameter is within 7.7–8.04, suggesting that in the case of solid solution formation, phases with both b.c.c. and f.c.c. lattices are possible.

Calculation using Taylor series of the liquidus temperature of selected NiCoCrAl–(Ti, Nb) alloys determined that, to achieve the required liquidus temperature (not higher than 1220–1230°C), the total content of Ti + Nb should be at least 16 at.% (Fig. 3).

According to the calculated data, the selected experimental alloys will exhibit a mixed structure, consisting of a solid solution based on nickel and intermetallic compounds based on  $Ni_3(Al, Ti, Nb)$ , with an acceptable calculated melting temperature  $T_{liq} = 1215^\circ\text{C}$  (Table 3). This renders them suitable for use as brazing filler metals for heat-resistant nickel alloys.

Further experimental studies, particularly x-ray microspectral analysis, confirmed that the alloy in its cast state comprises dendrites of two primary phases and some amount of interdendritic eutectic. The first phase, based on the Ni–Co system enriched with aluminium and titanium (Phase 1, Fig. 4), constitutes approximately 65% of the volume. The second phase, based on the Cr–Co–Ni system with a small

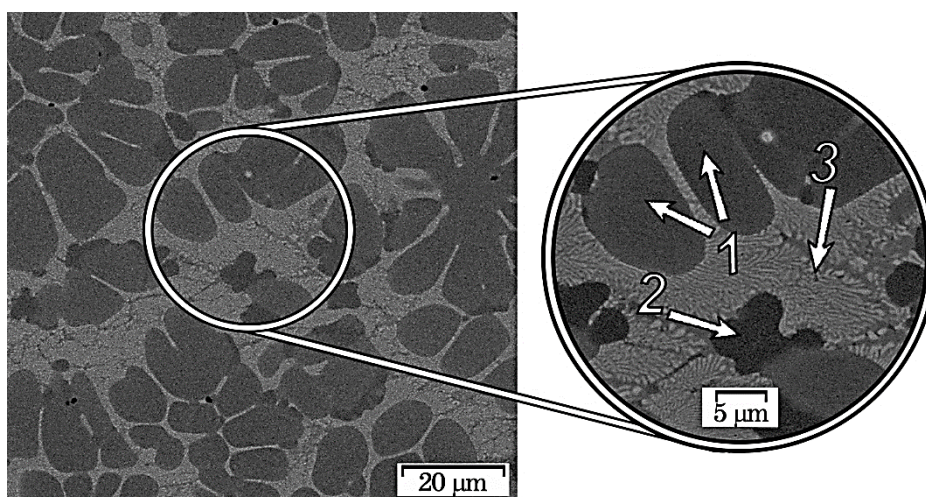


Fig. 4. Cross-sectional microstructure of the cast  $\text{Ni}_x\text{CoCrAl-Ti}_y\text{Nb}_z$  high-entropy alloy.

amount of aluminium, titanium, and niobium (Phase 2, Fig. 4), constitutes around 10% of the volume.

In the interdendritic spaces, eutectics formed by compounds enriched in aluminium, titanium, and niobium crystallize (Phase 3, Fig. 4). According to binary state diagrams, such compounds are formed because of a eutectic reaction during the crystallization of a liquid alloy [44].

#### 4. CONCLUSIONS

The results of calculations and analysis of state diagrams of metal systems indicate that the  $\text{NiCoCrAl-(Ti, Nb)}$  system is potentially promising for creating high-entropy solders for brazing Ni-based alloys. Using the calculation method, it was established that the values of the entropy of mixing ( $\Delta S_m$ ) as well as enthalpy of mixing ( $\Delta H_m$ ) and the atomic radii mismatch ( $\delta$ ) for this alloys correspond to the criteria put forward for high-entropy alloys.

Calculation using Taylor and Maclaurin series of the liquidus temperature of  $\text{NiCoCrAl-(Ti, Nb)}$  system alloys made it possible to determine that, to achieve a liquidus temperature not higher than 1220–1230°C, the total content of Ti + Nb should be at least 16 at.%.

Based on the findings from micro-x-ray spectral studies, it was determined that the selected experimental alloy  $\text{Ni}_x\text{CoCrAl-Ti}_y\text{Nb}_z$  exhibits Ni–Co dendritic components, enriched with aluminium and titanium, as well as Cr–Co–Ni-based components doped with small amounts

of aluminium, titanium, and niobium. Simultaneously, a small volume of the eutectic component of the formed compound, enriched with aluminium, titanium, and niobium, is present in the interdendritic spaces.

## REFERENCES

1. L. Hardwick, P. Rodgers, E. Pickering, and R. Goodall, *Metall. Mater. Trans. A*, **52**: 2534 (2021).
2. D. Kay, *Industrial Heating*, **70**, No. 11: 33 (2003).
3. D. Luo, Y. Xiao, L. Hardwick, R. Snell, M. Way, X. Sanuy Morell, F. Livera, N. Ludford, C. Panwisawas, H. Dong, and R. Goodall, *Entropy*, **23**, No. 1: 78 (2021).
4. A. Rabinkin, *Sci. Technol. Weld. Joining*, **9**, No. 3: 181 (2004).
5. S. B. Byelikov and A. D. Koval', *Metaloznavstvo ta Obrobka Metaliv*, No. 2: 20 (1995) (in Ukrainian).
6. S. Maksymova, V. Voronov, and P. Kovalchuk, *Metallofiz. Noveishie Tekhnol.*, **41**, No. 11: 1539 (2019) (in Russian).
7. X. Huang, *Weld. J.*, **93**, No. 7: 232 (2014).
8. M. Salmaliyan and M. Shamanian, *Heat Mass Transf.*, **55**, No. 8: 2083 (2019).
9. X. J. Yuan, M. B. Kim, and C. Y. Kang, *Mater. Sci. Technol.*, **27**, No. 7: 1191 (2011).
10. M. Abdelfatah and O. A. Ojo, *Mater. Sci. Technol.*, **25**, No. 1: 61 (2009).
11. J. W. Yeh, *J. Occup. Med.*, **65**: 1759 (2013).
12. M. Way, D. Luo, R. Tuley, and R. Goodall, *J. Alloys Compd.*, **858**: 157750 (2021).
13. S. V. Maksymova and V. E. Sukhoyars'kyi, *Metallofiz. Noveishie Tekhnol.*, **45**, No. 1: 75 (2023) (in Ukrainian).
14. B. Cantor, I. T. H. Chang, P. Knight, and A. J. B. Vincent, *Mater. Sci. Eng. A*, **375–377**: 213 (2004).
15. T. T. Zuo, L. Ouyang, X. Yang, Y. Cheng, R. Feng, S. Chen, P. Liaw, J. Hawk, and Y. Zhang, *Acta Mater.*, **130**: 10 (2017).
16. W. Tillmann, T. Ullitzka, L. Wojarski, M. Manka, H. Ullitzka, and D. Wagstyl, *Weld. World*, **64**: 201 (2020).
17. W. Tillmann, T. Wojarski, D. Stangier, M. Manka, and C. Timmer, *Weld. World*, **64**: 1597 (2020).
18. S. A. Firstov, V. F. Gorban', A. O. Andreev, and N. A. Krapivka, *Nauka ta Innovatsiyi*, **9**, No. 5: 32 (2013) (in Russian).
19. J. Yeh, *Annales De Chimie – Science des Matériaux*, **31**: 633 (2006).
20. G. S. Firstov, Yu. M. Koval, V. S. Filatova, V. V. Odnosum, G. Gerstein, and H. J. Maier, *Prog. Phys. Met.*, **24**, No. 4: 819 (2023).
21. S. I. Mudryj, R. M. Bilyk, R. Ye. Ovsyanyk, O. O. Kulyk, and T. M. Mika, *Phys. Chem. Solid St.*, **20**, No 4: 432 (2019) (in Ukrainian).
22. L. Jiang, Z. Q. Cao, J. C. Jie, J. J. Zhang, Y. P. Lu, T. M. Wang, and T. J. Li, *J. Alloy. Compd.*, **649**: 585 (2015).
23. S. Singh, N. Wanderka, B. S. Murty, U. Glatzel, and J. Banhart, *Acta Mater.*, **59**, No. 1: 182 (2011).
24. C. Y. Cheng and J. W. Yeh, *Mater. Lett.*, **181**: 223 (2016).

25. A. Manzoni, H. Daoud, R. Volkl, U. Glatzel, and N. Wanderka, *Ultramicroscopy*, **163**: 184 (2013).
26. Y. Lu, Y. Dong, S. Guo, L. Jiang, H. Kang, T. Wang, B. Wen, Z. Wang, J. Jie, Z. Cao, H. Ruan, and T. Li, *Sci Rep.*, **4**: 6200 (2014).
27. M. Mukarram, M. Mujahid, and K. Yaqoob, *J. Mater. Res. Technol.*, **10**: 1243 (2021).
28. H. Jiang, K. Han, X. Gao, Y. Lu, Z. Cao, M. C. Gao, J. A. Hawk, and T. Li, *Mater. Des.*, **142**: 101 (2018).
29. Y. P. Lu, X. Z. Gao, L. Jiang, Z. N. Chen, T. M. Wang, J. C. Jie, H. J. Kang, Y. B. Zhang, S. Guo, H. H. Ruan, Y. H. Zhao, Z. Q. Cao, and T. J. Li, *Acta Mater.*, **124**: 143 (2017).
30. I. S. Wani, T. Bhattacharjee, S. Sheikh, P. P. Bhattacharjee, S. Guo, and N. Tsuji, *Mater. Sci. Eng. A*, **675**: 99 (2016).
31. S. Guo and C. Liu, *Prog. Nat. Sci.: Mater. Int.*, **21**, No. 6: 433 (2011).
32. B. Vishwanadh, N. Sarkar, S. Gangil, S. Singh, R. Tewari, G.K. Dey, and S. Banerjee, *Scr. Mater.*, **124**, No. 11: 146 (2016).
33. X. Sun, H. Zhang, S. Lu, X. Ding, Y. Wang, and L. Vitos, *Acta Mater.*, **140**, No. 5: 366 (2017).
34. Y. Zhang, Z. P. Lu, S. G. Ma, P. K. Liaw, Z. Tang, Y. Q. Cheng, and M. C. Gao, *MRS Communications*, **4**, No. 2: 57 (2014).
35. M. C. Gao, J.-W. Yeh, P.K. Liaw, and Y. Zhang, *High-Entropy Alloys* (Switzerland: Springer International Publishing: 2016).
36. Y. Zhang, T. T. Zuo, Z. Tang, M. C. Gao, K. A. Dahmen, P. K. Liaw, and Z. P. Lu, *Prog. Mater. Sci.*, **61**: 1 (2014).
37. A. K. Singh, K. Kumar, A. Dwivedi, and A. Subramaniam, *Intermetallic*, **53**: 112 (2014).
38. V. G. Ivanchenko, S. P Oshkad'orov, and S. M. Severyna, *Metaloznavstvo ta Obrobka Metaliv*, **1**: 21 (2014) (in Ukrainian).
39. A. Takeuchi and A. Inoue, *Mater. Trans.*, **46**, No. 12: 2817 (2005).
40. M. Ren, B. S. Li, and H. Z. Fu, *Trans. Nonferrous Met. Soc. China*, **4**: 991 (2013).
41. S. A. Firstov, V. F. Gorban', N. A. Krapivka, N. Y. Danylenko, and V. N. Nazarenko, *Voprosy Atomnoi Nauki i Tekhniki*, **2**: 178 (2015) (in Russian).
42. L. Jiang, Y. P. Lu, H. Jiang, T. M. Wang, B. N. Wei, Z. Q. Cao, and T. J. Li, *Mater. Sci. Technol.*, **32**, No. 6: 588 (2016).
43. S. Guo, C. Ng, J. Lu, and C. T. Liu, *J. Appl. Phys.*, **109**: 103505 (2011).
44. T. B. Massalski, *Binary Alloy Phase Diagrams* (Metals Park, Ohio: ASM International: 1990) (in CD).